Atomistic simulation of transport properties of non-graphitic armchair nanotubes and effect of Stone-Wales defects

Amretashis Sengupta

Hanse-Wissenschaftskolleg,
Lehmkuhlenbusch 4,
27753 Delmenhorst, Germany
amretashis@gmail.com

School of VLSI Technology,
IIEST, Shibpur,
Howrah – 711 103, India
dr.a.sengupta@ieee.org

***Abstract*—In this work, we study the carrier transport properties of three non-graphitic armchair nanotubes (of Silicene, Germanene and Phosphorene) under an empirical tight binding (ETB)– non-equilibrium Green's function (NEGF) approach. The electronic properties are studied with extended Hückel theory, while phonon calculations are carried out with Stillinger-Weber classical potentials in ATK. The impact of Stone-Wales (SW) defects in electron and phonon transport properties of such tubes is also investigated. Our simulations show Silicene and Germanene nanotubes to offer much better electrical conduction than phosphorene NTs. The carrier transport and change charge density around the SW defect site is found to be affected more significantly in phosphorene nanotubes. Suppression of phonon transmission with introduction of defect is observed for all the cases. The overall results show a good possibility of defect engineered tailoring of electrical and thermal properties of these nanotubes.**

Keywords—nanotubes, defect, ETB, NEGF, phonon

I. Introduction

Nanotubes of non-graphitic 2 D materials such as Silicene, Germanene, MoS_2 and Phosphorene are beginning to generate significant interest of late owing to their mechanical, optical and electronic properties [1]-[3]. Also for nanoelectronics applications such tubes hold good promise as nanotube FETs or interconnect materials. The atomistic simulation of the electronic transport properties of such nanotubes (NTs) could therefore be of considerable importance for device applications. In this work we investigate by empirical tight binding (ETB) methods carrier transport (device density of states (DDOS), carrier densities, I-V characteristics), phonon transmission and thermoelectric properties of armchair nanotubes of Silicene, Germanene and Phosphorene. As the honeycomb structure of the 2D lattice of Silicene, Germanene and Phosphorene are susceptible to Stone-Wales (SW) defects [3,4], we further study their impact on the carrier transport properties of these NTs.

II. Methodology

The armchair nanotubes (of diameters ~ 2 nm) are considered consisting of a central (device) region connected to left and right electrodes extending to reservoirs far away (where the bias is applied). For the ETB study we use a 1x1x50 Monkhorst-Pack k-grid [5] on the device supercell and employ the extended Hückel theory (EHT). EHT is chosen for the simulations owing to its computational efficiency for simulating large device supercells, as compared to density functional theory (DFT) and good estimation of electronic band-gaps. [7] We use the Hoffman basis sets for Si, Ge and P with vacuum energy level of 0 eV in all three cases. [6,7] The Wolfsburg weighting scheme is used in our extended Hückel theory calculations. Mesh cutoff energy of 10 Ha is used with the Pulay-mixer algorithm as iteration control parameter and tolerance value of 10^{-5} Ha. [8]

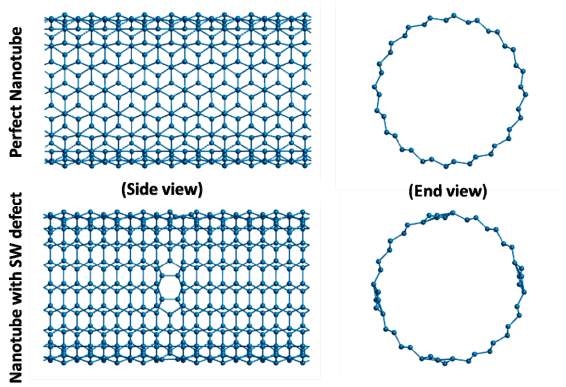

Fig. 1. Perfect nanotubes and nanotube containing Stone-Wales defect under study. Defects are considered only in the central region of device simulation.

Non-equilibrium Green's function (NEGF) transport in ATK, is simulated with a multi-grid Poisson solver for the device configuration using Dirichlet boundary conditions on the electrodes (i.e. left and right faces) and Neumann boundary conditions on the other faces of the device supercell. [6,9] Krylov self-energy calculator is used for the transmission calculations, with the average Fermi level set as the energy zero parameter. A perturbation magnitude of 10^{-6} is considered for correct calculation of the retarded Green's function matrix. The two probe ballistic current is evaluated as [6,7,9]

$$I = \left(\frac{g_S g_v e}{h}\right)\int_{-\infty}^{+\infty} \Im(E)\left[f_L\left(E_{k,x}-\eta_L\right)-f_R\left(E_{k,x}-\eta_R\right)\right]dE \quad (1)$$

In (1) e is the electronic charge, h is the Planck's constant, $\Im$ is the transmission, $f_{L,R}$ are the Fermi functions in

978-1-5090-0818-6/16/$31.00 ©2016 IEEE

the left and right contacts respectively, $\eta_{L,R}$ are the left and right contact chemical potentials respectively. $g_{s,v}$ are the spin degeneracy and valley degeneracy respectively, $E_{k,x}$ the energy eigenvalue.

The calculations for phonons is carried out with Stillinger-Weber classical potentials (for Si, Ge NTs) and EAM_NiP_Sheng classical potential (for P NTs) [10,11] using the frozen phonon method which is a supercell based small displacement calculation. [6,12] 180 small displacements each of 0.01 Å value are applied in the c direction of the device supercell for calculating forces and the dynamical matrix of the system, which is used in calculating the phonon properties. The contribution of both electrons and phonons are taken into account for calculating the heat current I_Q due to voltage/ temperature difference between the electrodes, and thus the thermal conductance is evaluated as [13,14]

$$\kappa = \left.\frac{dI_Q}{dT}\right|_{I=0} \tag{2}$$

thermoelectric figure of merit (ZT) is calculated as [13]

$$ZT = \frac{\wp_e \mathbb{S}^2 T}{\kappa} \tag{3}$$

In (3), $\wp_e$ is the electrical conductance, $\mathbb{S}$ the Seebeck coefficient, T is the temperature.

III. Results and Discussions

From the projected device DOS (Fig. 2), the density of up and down spin conduction channels seem symmetric. Larger number of states are seen below the fermi level (ε_F=0), than above it for Si and Ge NTs. States are further away from the fermi level in case of phosphorene NT. With the incorporation of Stone-Wales defect, there seems a marked increase in magnitude as well as broadening of device DOS, for Si and Ge NTs. For phosphorene NTs, the broadening is present but in slightly lesser amount, although peaks are significantly strengthened more than Si and Ge NTs. A direct band gap of ~ 0.32 eV and 0.18 eV is calculated for perfect Si and Ge NTs, for P NTs this is indirect gap of about 1.79 eV. The effect of these defects are more prominently observable in terms of electron density projections (shown in Fig. 3). For the perfect NTs, the projected carrier density along the c-axis remains almost fixed around values n_e ~305 Å^{-3} for Si NT, n_e ~ 289.5 Å^{-3} for Ge NT and n_e ~455.5 Å^{-3} for P NT. In presence of SW defects, there is a sharp undulation in n_e around the region where the defect is created. At the center of the defect site, a dip in n_e by ~ 10 Å^{-3}, is seen for Si and Ge NTs, for P NT this dip is about 20 Å^{-3}. In the sites adjacent to the SW defect a rise in n_e is observed (~ 5 Å^{-3} for Si and Ge NTs, and ~ 10 Å^{-3} for P NT). This shows a stronger defect induced carrier density redistribution for phosphorene NT. This could be owing to stronger changes in the *s* and the *p* orbital contribution of the atoms around the defect site to the overall density of states in P NTs, as compared to that in Si and Ge NTs.

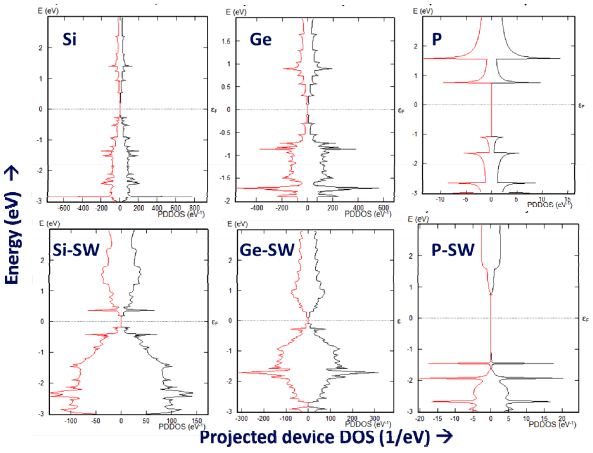

Fig. 2. Projected device density of states for the various NTs under study. Both up (+ve side of *x*) and down spin conduction states are shown in the figure (+ve side of *x*)

The current voltage (I-V) characteristics are shown in Fig. 4. Si and Ge NTs show much higher currents in the range of ~ 300 - 350 μA, compared to P NTs (I ~ 1-8 μA). This can be explained by the near metallic behavior of Si and Ge NTs with smaller band gaps and lesser carrier effective masses compared to P NTs. In presence of SW defects the current in P NT seems to be enhanced greatly after V=2 Volts, as the strong DDOS peaks (Fig. 2) around -1eV and less, start to fall within the bias window with increasing voltage. For Si and Ge the current enhancement is not that significant in presence of defect states.

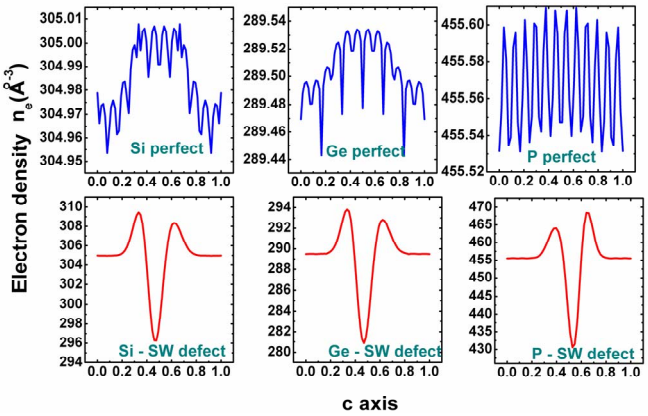

Fig. 3. Electron densities projected on to the c-axis of the various NTs.

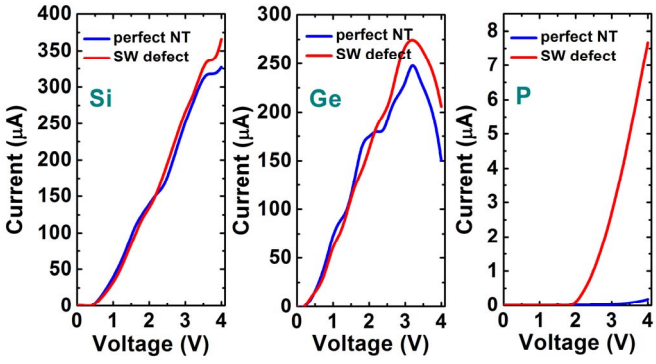

Fig. 4. Simulated I-V characteristics of the various NTs.

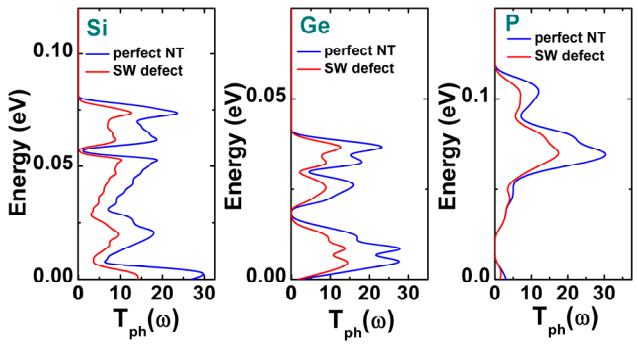

Fig. 5. Simulated phonon transmission characteristics of the various NTs.

The phonon transmission spectra (Fig. 5), shows multiple peaks in T_{ph} for Si and Ge NTs and a single less sharper (in comparison) peak for P NT. It also indicates that a considerable quenching of phonon transmission in presence of SW defects for all the three NTs. In Fig. 6 we show the thermal conductance, considering the contributions of both electrons and phonons to the heat current. The simulation results at 300 K, show Si and Ge NTs to have a higher value of κ_{e+ph} as compared to P NT. In case of the Si and Ge NTs, the heat transport coefficient is electronic conduction dominated for a larger range of 0 - 3 eV than P NTs where this range is about 0.75 - 3 eV. Si and Ge NTs also show a peak of the coefficient at about 1.1 and 1.2 eV respectively, the value of this peak being slightly higher for Si (~13.75 nW/K) than Ge (~11.9 nW/K). For P NT a plateau is observed for the maximum κ_{e+ph} ~4.55 nW/K, in the range of 1.75 – 3 eV. In the presence of the SW defects, κ is significantly reduced to ~40-50% of their original (perfect) values. A constriction of the electronic conduction dominated range is also observed, which is most prominent for P NTs.

The calculated thermoelectric parameters namely conductance ($\wp_e$), Peltier coefficient (Π) and Seebeck coefficient ($\mathbb{S}$) at T=300K, are listed in Table -I. It is notable that there is a change of sign in the Seebeck and Peltier coefficients in Ge NT upon the introduction of defect. This suggests a change from electron dominated to hole dominated heat conduction with SW defect in Ge NT. For P NT the heat conduction is hole dominated for both perfect and defect cases, while for Si NT its electron dominated for both.

TABLE I. CALCULATED THERMOELECTRIC PARAMETERS (T=300K)

Material	Thermoelectric parameters		
	$\wp_e$ *(S)*	Π *(V)*	$\mathbb{S}$ *(V/K)*
Si NT perefct	1.970×10^{-7}	-4.325×10^{-3}	-1.442×10^{-5}
Si NT SW defect	1.336×10^{-7}	-1.106×10^{-2}	-3.685×10^{-5}
Ge NT perfect	4.240×10^{-6}	-7.627×10^{-5}	-2.542×10^{-7}
Ge NT SW defect	2.391×10^{-6}	5.320×10^{-3}	1.775×10^{-5}
P NT perfect	3.802×10^{-17}	7.771×10^{-1}	2.590×10^{-3}
P NT SW defect	3.590×10^{-19}	8.037×10^{-1}	2.676×10^{-3}

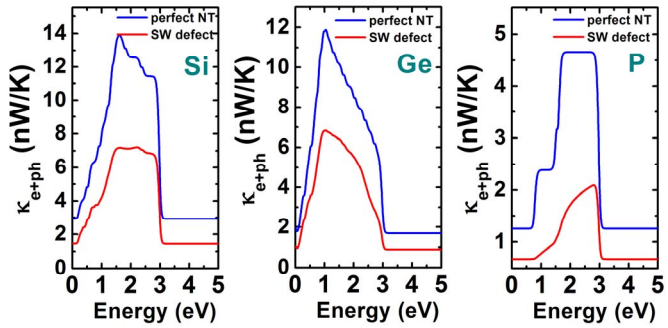

Fig. 6. Simulated thermal conductance (at T=300K) for the various NTs.

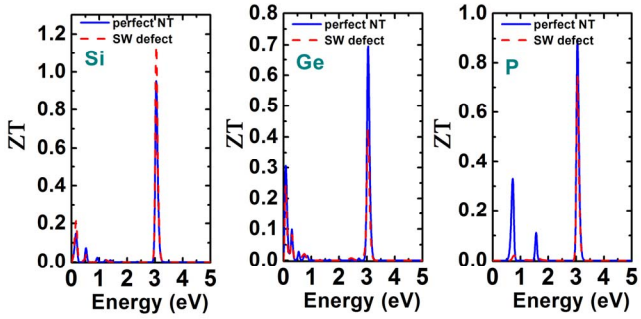

Fig. 7. Simulated thermoelectric figure of merit (at T=300K) for the various NTs.

The calculated thermoelectric figure of merit (*ZT*) is shown in Fig. 7. In all the three cases of perfect NTs, a strong peak is observed around 3 eV, followed by less stronger peaks in 0.25, 0.7 eV for Si, 0.1,0.3 eV for Ge and 0.85, 1.65 eV for P NTs. In the presence of defects, in P NT the peaks in ZT below 3 eV seem to be suppressed, more significantly those around 0.85 and 1.65 eV. For Ge NT with SW defect, the peaks are suppressed due to SW defect as well. For Si NT however, the defects seem to significantly enhance the peak at 3 eV and also slightly enhance the peak around 0.25 eV, others remaining almost unchanged. This peculiar behavior of enhancement of ZT peaks in Si NT due to SW defects may be explained by the increase in the Seebeck coefficient from -1.442×10^{-5} to -3.685×10^{-5} V/K compared to that of the perfect Si NT.

IV. CONCLUSION

From the simulations it is seen Silicene and Germanene NTs show more metallic behavior than phosphorene NTs and conduct higher currents. However phosphorene NTs undergo more significant carrier density redistribution around the Stone-Wales defects. The enhancement of current, quenching of phonon transmission, and significant variations in thermoelectric parameters indicate significant possibility of defect engineered tailoring of electrical and thermal transport properties in these armchair nanotubes.

ACKNOWLEDGMENT

The author thanks DST for Grant No. IFA-13 ENG-62, and Hanse-Wissenschatskolleg foundation for the HWK fellowship 2016-17.

REFERENCES

[1] H. Guo, N. Lu, J. Dai, X. Wu, and X. C. Zeng, "Phosphorene nanoribbons, Phosphorus nanotubes, and van der Waals Multilayers," J. Phys. Chem. C, vol. 118, pp. 14051–14059, June 2014.

[2] X. Li, S. Wu, S. Zhou, and Z. Zhu, "Structural and electronic properties of germanene/MoS2 monolayer and silicene/MoS2 monolayer superlattices.," Nanoscale Res. Lett., vol. 9, pp. 110 1-9, March 2014.

[3] C. H. Zhang, Q. Ran, and J. Shen, "Structural stability of silicene-like nanotubes," Comput. Phys. Commun., vol. 183, no. 1, pp. 30–33, January 2012.

[4] H. Sahin, J. Sivek, S. Li, B. Partoens, and F.M. Peeters, "Stone-Wales defects in silicene: Formation, stability, and reactivity of defect sites," Phys. Rev. B, vol. 88, Issue 4, pp. 045434-1– 045434-6 , July 2013.

[5] H. J. Monkhorst, and J. D. Pack, "Special points for Brillouin-zone integrations," Phys. Rev. B, vol. 13, pp. 5188 – 5192, June 1976.

[6] QuantumWise Atomistix Tool Kit (ATK) Manual v2015.1 [Online] http://www.quantumwise.com/documents/manuals/latest/ReferenceManual/index.html/

[7] K. Stokbro, D.E. Petersen, S. Smidstrup, A. Blom, M. Ipsen, and K. Kaasbjerg, "Semiempirical model for nanoscale device simulations," Phys. Rev. B, vol. 82, pp. 075420-1 – 075420-7, August 2010.

[8] P. Pulay, "Convergence acceleration of iterative sequences the case of SCF iteration," Chem. Phys. Lett., vol. 73, no. 2, pp. 393–398, Jul. 1980.

[9] M. Luisier and G. Klimeck, "Simulation of nanowire tunneling transistors: From the Wentzel-Kramers- Brillouin approximation to full-band phonon-assisted tunneling," J. Appl. Phys., vol. 107, no. 8, pp. 084507-1 – 084507-6, April 2010.

[10] M. Laradji, D.P. Landau, and B. Dünweg, " Structural properties of Si 1-x Ge x alloys: A Monte Carlo simulation with the Stillinger-Weber potential," Phys. Rev. B, vol. 51, pp. 4894 – 4902, February 1995.

[11] H.W. Sheng, M.J. Kramer, A. Cadien, T. Fujita, and M.W. Chen, "Highly optimized embedded-atom-method potentials for fourteen fcc metals," Phys. Rev. B, vol. 83, pp. 134118-1–134118-20, April 2011.

[12] K. Kaasbjerg, K.S. Thygesen, and K.W. Jacobsen, "Phonon-limited mobility in n-type single-layer MoS 2 from first principles," Phys. Rev. B, vol. 85, pp.115317-1 – 115317-16, March 2012.

[13] T. Markussen, A.-P. Jauho , and M. Brandbyge, "Surface-decorated Silicon nanowires: A route to high-ZT thermoelectrics," Phys. Rev. Lett., vol. 103, pp. 055502-1–055502-4, July 2009.

[14] Y. Cai, J. Lan, G. Zhang, and Y-W. Zhang, "Lattice vibrational modes and phonon thermal conductivity of monolayer MoS2," Phys. Rev. B, vol. 89, pp. 035438-1 – 035438-8, Januray 2014.